Theory of Piezotronics and Piezo-phototronics

Yan Zhang [1,2], Yongsheng Leng [3], Morten Willatzen [2, 4], and Bolong Huang [5]

[1] School of Physics, University of Electronic Science and Technology of China, Chengdu 610054, China;

[2] Beijing Institute of Nanoenergy and Nanosystems, Chinese Academy of Sciences; College of Nanoscience and Technology, University of Chinese Academy of Sciences, Beijing 100049, China;

[3] Department of Mechanical and Aerospace Engineering, The George Washington University, Washington, DC 20052, USA;

[4] Department of Photonics Engineering, Technical University of Denmark;

[5] Bolong Huang, Department of Applied Biology & Chemical Technology, The Hong Kong Polytechnic University;

* E-mail: zhangyan@uestc.edu.cn, leng@gwu.edu, morwi@fotonik.dtu.dk, and bhuang@polyu.edu.hk

Abstract

Piezotronic and piezo-phototronic devices exhibit high-performance and potential applications in next generation self-powered, flexible electronics and wearable systems. Strain-induced piezoelectric field at junction, contact, or interface can significantly modulate the carrier generation, recombination, and transport properties. This mechanism has been studied based on theory of piezotronics and piezo-phototronics. Simulation-driven material design and device improvement have been greatly propelled by finite element method, density functional theory and molecular dynamics for achieving high-performance devices. Dynamical piezoelectric field also can control new quantum states in quantum materials, for example, topological insulators, which pave new path for enhancing performance and investigate fundamental physics of quantum piezotronics and piezo-phototronics.

Introduction

Piezotronics and piezo-phototronics are emerging fields by coupling piezoelectricity, semiconductor, and photon excitation for achieving high-performance devices [1-3], such as nanogenerators [4-6], piezotronic field-effect transistors [7], strain sensor [8], LEDs [9], solar cells [10], strain-gated taxel-addressable matrices [11], piezo-phototronic strain sensor arrays [12], two-dimensional piezotronic transistor [13], and strain-gated logic devices [14]. The built-in piezoelectric potential effectively controls carrier transport characteristics in piezoelectric semiconductors [15-18], such as ZnO, GaN, InN, CdS and monolayer MoS_2.

The first piezotronic strain sensor fabricated by ZnO nanowire shows high strain sensitivity that the gauge factor reaches up to 1250 [8]. Strain-induced piezoelectric potential modulates the properties of carrier transport, generation, and recombination at junction or interface of semiconductor. There are two novel features of piezotronic and piezo-phototronic devices: one feature is that piezoelectric materials convert mechanical stimuli to electric signal; other feature is that strain-induced piezoelectric charges directly control carriers in depletion layer of p-n junction or metal-semiconductor contact, which amplifies the piezoelectric signal. Therefore, the high sensitivity mechanism is that piezotronic transistors simultaneously have energy/signal conversion and amplification functions.

In particular, piezotronic and piezo-phototronic devices exhibit novel properties of sensitivity enhancement for strain sensing applications [8, 19] and energy conversion improvement for solar cells [10, 20]. According to semiconductor physics and piezoelectric theory, fundamental piezotronic theory had been established, and piezotronic p-n junction and metal-semiconductor contact models have been constructed [15, 18]. Piezotronic and piezo-phototronic effects provide fundamental understanding on the results of previous theoretical and experimental works, for example, piezopotential modulates the Schottky barrier heights (SBHs) at the metal-semiconductor contacts [21], changes electric field distribution in CdS-based photovoltaic [22], and separates photon-induced electron-hole pairs in core-shell structure [23].

Coupling properties can be used to convert the mechanical or optical signal to ON or OFF output signals. Piezotronic logic devices based on the strain-gated transistors had been fabricated for logic units of NAND, NOR, and XOR [4] and piezo-phototronic binary computation by piezoelectric semiconductor by wurtzite structure ZnO and CdS [8]. Piezotronic transistors can be strain sensors, signal comparators and amplifiers, which designed novel piezotronic analog-to-digital converters (ADCs) for conversion from a continuous-time and -amplitude analog signal to a discrete-time and -amplitude digital signal in strain mapping and digital processing [24]. The piezo-phototronics mainly involves the generation and recombination properties of the carriers

which can be controlled by strain-induced piezoelectric charges [16, 18]. Various high performance piezo-phototronic devices such as solar cell [10, 20], LED [9] and piezo-phototronic photocell [25] have been developed. Piezotronic nanodevices with high strain sensitivity, fast response, and low power consumption are good candidates for internet of things and self-powered applications. Above works provide not only the deep understanding on piezotronic and piezo-phototronic effects, but also guidance for developing high-performance devices.

Fundamental Theory and Device Physics of Piezotronics and Piezo-phototronics

Piezotronic and piezo-phototronic devices had been described by semiconductor physics [26] and piezoelectric theory [27]. Basic equations are electrostatic, current-density, continuity, and piezoelectric equations, which are utilized for characterizing charge carriers transport behaviors and the interaction of photon-electron under piezoelectric field induced by dynamic straining.

Poisson equation, one of Maxwell equations, describes the charge induced potential distribution in piezotronic and piezo-phototronic devices:

$$\nabla^2 \psi_i = -\frac{\rho(\vec{r})}{\varepsilon_s} \tag{1}$$

where ψ_i , $\rho(\vec{r})$ and ε_s are the potential, the charge density, and the dielectric coefficient.

The current-density equations describe drift and diffusion current density for steady state conditions:

$$\begin{cases} \mathbf{J_n} = q\mu_n n\mathbf{E} + qD_n \nabla n \\ \mathbf{J_p} = q\mu_p p\mathbf{E} - qD_p \nabla p \\ \mathbf{J} = \mathbf{J_n} + \mathbf{J_p} \end{cases} \tag{2}$$

where $\mathbf{J_n}$, $\mathbf{J_p}$ and $\mathbf{J}$ are the electron, hole and total current densities, q is unit electronic charge, electron and hole mobility are μ_n and μ_p, free electrons and holes concentrations are n and p , $\mathbf{E}$ is electric field, electrons and holes diffusion coefficients are D_n and D_p , respectively.

The time-dependent phenomena are described by the continuity equations for generation and recombination:

$$\begin{cases} \dfrac{\partial n}{\partial t} = G_n - U_n + \dfrac{1}{q}\nabla \cdot \mathbf{J_n} \\ \dfrac{\partial p}{\partial t} = G_p - U_p - \dfrac{1}{q}\nabla \cdot \mathbf{J_p} \end{cases} \tag{3}$$

where G_n is electron generation rate, and G_p is hole generation rate, U_n and U_p are the recombination rates, respectively.

Applied a small uniform strain **S,** the polarization **P** is given by:[27]

$$(\mathbf{P})_i = (\mathbf{e})_{ijk}(\mathbf{S})_{jk} \tag{4}$$

where tensor $(\mathbf{e})_{ijk}$ is the piezoelectric coefficient.

The constitutive equations can be written as:[27-29]

$$\begin{cases} \boldsymbol{\sigma} = \mathbf{c_E S} - \mathbf{e^T E} \\ \mathbf{D} = \mathbf{eS} + \mathbf{kE} \end{cases} \tag{5}$$

where tensor $\boldsymbol{\sigma}$ and $\mathbf{c_E}$ are the stress and elasticity. $\mathbf{D}$ is the electric displacement. $\mathbf{k}$ is the dielectric tensor.

Piezopotential can change the energy band. The schematic of piezotronic transistor is shown in Figure 1(a). For one-dimensional p-n junction, the built-in potential ψ_{bi} is obtained as:

$$\psi_{bi} = \frac{q}{2\varepsilon_s}(N_A {W_{Dp}}^2 + \rho_{piezo} {W_{piezo}}^2 + N_D {W_{Dn}}^2) \tag{6}$$

where N_A and N_D are the acceptor and donor concentrations, ρ_{piezo} is of piezoelectric charge number density, *Wpiezo* is a width of uniform piezoelectric charge distribution, W_{Dp} and W_{Dn} are p-side and the n-side depletion layer lengths, respectively.

Current-voltage characteristic of the piezotronic p-n junction or metal-semiconductor contact is given by:

$$J = J_0 \exp(\frac{q^2 \rho_{piezo} {W_{piezo}}^2}{2\varepsilon_s kT})[\exp(\frac{qV}{kT}) - 1] \tag{7}$$

where J_0 is the saturation current density, which is J_{C0} for p-n junction or J_{D0} for metal-semiconductor contact:

$$J_{C0} = \frac{qD_p n_i}{L_p}\exp(\frac{E_i - E_{F0}}{kT}) \tag{8}$$

where L_p is hole diffusion length, n_i and E_i are the intrinsic carrier density and Fermi level,

E_{F0} is Fermi level without piezoelectric charges.

$$J_{D0} = \frac{q^2 D_n N_C}{kT} \sqrt{\frac{2qN_D(\psi_{bi0} - V)}{\varepsilon_s}} \exp(-\frac{q\phi_{Bn0}}{kT}) \quad (9)$$

where N_C is the effective density of states at the conduction band, ϕ_{Bn0} is Schottky barrier height without piezoelectric charges.

The current is an exponential function of strain-induced charges, which can be effectively controlled by tensile or compressive strain. The current-voltage curves of piezotronic metal-semiconductor contact are shown in figure 1(b). Furthermore, the piezotronics PIN structure diode has been demonstrated for high-frequency applications in microwave devices [30]. Considering dynamics properties of high frequency strain, piezotronic and piezo-phototronic devices may broaden the conventional applications beyond the statics features [31]. Piezotronic effect on semi-classical ballistic transport prosperities can be studied by classical Boltzmann equation [32]. For monolayer MoS_2, the band structure can be calculated by Schrodinger equation, which is given as:

$$\left(-\frac{\hbar^2}{2m_Z} \frac{\partial^2}{\partial z^2} + qV \right) \psi_{n_z} = E_{n_z} \psi_{n_z} \quad n_z = 1, 2, 3, ... \quad (9)$$

where ψ_{n_z} is the wavefunction, E_{n_z} is energy level, n_z is the quantum number, m_z is effective mass of electron. The potential V include the effect of piezo-charges.

Piezoelectric charges changing wavelength and enhancing luminescence performance in quantum devices have received extensive researches for wurtzite structure ZnO nanowire, monolayer MoS_2 and CdTe quantum dot [24, 33-35]. The coupling between piezo-phototronics effect and surface plasmonic resonance has been explored both in theoretically and experimentally and can be used to remarkably enhance the photoluminescence in InGaN/GaN quantum well [36]. In addition, a self-consistent numerical model in the energy realignment realized by strain-induced piezoelectric charges has been investigated in InGaN/GaN quantum well aiming at clarifying the high performance of solar cell [37].

Simulation-driven material design and device improvement for Piezotronics and Piezo-phototronics

Piezotronics and piezo-phototronics strongly stimulated research on material design and device improvement, which offer atomistic calculations and semiconductor device simulation. For one success example, two back-to-back bulk ZnO with reversely growing directions increase piezoelectric charge density, the material and device have been realized experimentally with a

great gauge factor approaching to 800 [38]. Another example is size effect on mechanical and piezoelectric properties of piezoelectric nanowire, which has been studied systematically by coupling of experimental and computational studies [39].

The complete set of all these semiconductor physics, material simulation, and device design techniques will establish the simulation-driven material design and device improvement for piezotronics and piezo-phototronics, as shown in Figure 2. Firstly, material properties can be obtained from material structural and elemental characterization. Secondly, atomistic calculations, such as **k·p** theory (**k** is the wavevector and **p** is the quantum-mechanical momentum operator), Density Functional Theory and molecular dynamics obtain the interface, semiconductor, and piezoelectric properties and compare the results of data from experiments. There are tremendous progress for calculations and simulations of material properties, which can guide and facilitate the design and optimization for piezotronic and piezo-phototronic devices. The development of software package is also required for the design and simulation of piezotronic and piezophototronic circuit, integrated chip, and sensor network . Artificial intelligence may provide powerful tools to develop new methods for search, discovery and optimization of piezotronic and piezo-phototronic materials.

Contact and Interface properties. Computational modeling of metal/ZnO contacts in piezotronic devices could be done by fully atomistic molecular dynamics (MD) simulations [40-42]. This is a crucial step to understand, from the viewpoint of simulation-driven material and device design, the structure and dynamics at interfaces and the dependence of device performance on various factors. For example, the Schottky barrier height at metal/ZnO contacts will depend on the size of contacts and the mechanical stability at the interface during repeated mechanical loadings [42]. Essentially, the total Hamiltonian of a metal/ZnO contact in a piezotronic device should include contributions from both the atomic contact at the interface and mechanical driving systems [42]. For example, in a sliding-bending piezoelectric nanogenerator, the total Hamiltonian at classical level should be a function of the positions and momenta of all the particles in the ZnO NW and metal tip, and the equivalent macroscopic position and momentum of the AFM cantilever system, together with the elastic potential energy of driving springs, as shown in Figure 3(a). Using MD simulation, acoustic transition radiation can be occurred due to the strain-induced polarization, which can sufficiently detect terahertz frequency strain wave with sub-picosecond level which approaches to atomic time and space resolution [43]. Classical core-shell interatomic potentials have been proposed to the study of piezoelectric properties for ZnO nanostructure by molecular dynamics and molecular statics [44]. Humidity effect on the piezoelectric and semiconductor properties has also been demonstrated in ZnO nanowires by MD

simulations [45]. Further, the piezoelectric constant in collagen is calculated with pC/N level which is in agreement with the experimental measurement [46].

Semiconductor properties. Pointing to the current demands of higher sensitivity and lower threshold of mechanical initiation for ZnO based piezotronic devices, the electronic properties of various ZnO systems had been studied, especially on the intrinsic defects determined dopable range for further flexible modulations of mechanically induced photoemission [47, 48]. The doping behaviors in material systems, e.g., ZnO, are important for designing piezotronic and piezo-phototronic devices[49]. Recent investigation shows that, with the dimension of the ZnO system decreasing instead of symmetry-decrease, ZnO becomes more and more flexible in suppressing local electron-phonon coupling via local lattice symmetrically relaxation. This is advantageous for adopting wider doping limit without spontaneously causing the intrinsic deep trapping defect, especially to complicated rare earth (RE) ions. That is the key that only the lower dimensional ZnO system can achieve bi-polar doping. Thus, 2D ZnO is a promising candidate to achieve a wider doping range in ZnO. The excited states of lanthanide (Ln) elements in both the divalent (Ln2+) and trivalent (Ln3+) state in such 2D-ZnO lattice were extensively studied. Trivalent Ln doping follows the removal of apical dominance concept, contributing more flexible energy transfer for photonic and electronic devices, as shown in Fig. 3(b). The Smith chart (Fig. 3b) can be used for simultaneously describing the photon-electronic excitation levels and corresponding oscillator strengths, in which energetic area has broadened with host electronic transition migrating from lattice vibration externally induced by local piezo-electrical field. This can potentially guide a selection or combination of multi-lanthanide-doping for designing the energy path for extra-low excitation-threshold to self-power driving system.

Piezoelectric properties. First principle calculations are widely used in previous works for calculating piezoelectric coefficients, or searching high piezoelectric response materials [50]. The width of piezoelectric charge distribution is important parameter which offers the band structure and interface engineering. According to the density functional theory, the width of piezoelectric charge distribution has been calculated in different metal and semiconductor transistors [51, 52], as shown in Figure 3(c)-(e). Piezoelectric properties of two-dimensional materials has also been outlined based on computational predictions and experimental characterization [53]. Piezoelectric potential and deformation potential simultaneously exist in the presence of mechanical strain, affecting the luminescence in InGaN/GaN quantum well [54]. It was demonstrated by Zhu et al. [55] and Wu et al. [13] that monolayer MoS_2 can exhibit high piezoelectric coefficients and power output. Piezoelectricity is allowed in MoS_2 containing an odd number of layers since these structures lack centrosymmetry but disappears in 2D MoS_2 with an even number of layers. It was

also concluded in Refs. [13, 55] that the piezoelectric coefficients of MoS_2 degrade rapidly with increasing number of layers for odd-layered structures. The piezoelectric constant e_{11} was experimentally found to be 2.9×10^{-10} C/m. Fei et al. [56] reported giant piezoelectric constants in monolayer SnSe, SnS, GSe, and GeS based on density-functional theory. For monolayer SnSe the computed piezoelectric constants were between 1 and 2 orders of magnitude larger than monolayer MoS2 and ZnO structures. The reason for the large piezoelectric coefficients was attributed to the unique "puckered" C_{2v} symmetry of the group-IV elements [56]. Other interesting novel piezoelectric materials for nanogenerator and sensing materials, that can be operated under harsh conditions and with a high Curie temperature Tc, are grain-oriented textured PbTiO3 ceramics where large piezoelectric voltage coefficients g_{33} are obtained via Sn and Mn doping due to a combination of a high d_{33} constant and a relatively small dielectric constant ε_{33} [57].

The understanding or prediction of materials' piezoelectric property can be facilitated by computation and modeling [58, 59]. Such bandstructures are provided by the **k·p** method which, in comparison with atomistic models, does not require increasing computational power with the number of atoms in the computational domain. Grundmann et al. [60] used the 8×8 **k·p** method to demonstrate a significant influence of piezoelectricity on the electronic eigenstates and optical properties of zincblende InAs/GaAs pyramidal quantum dot structures. Andreev and O'Reilly [61] used a multiband **k·p** theory to determine the influence of strain and piezoelectricity for the electronic bandstructure of GaN/AlN wurtzite quantum dots. Fonoberov and Balandin [62] used continuum elasticity theory and **k·p** theory to obtain excitonic properties of strained zincblende and wurtzite GaN/AlGaN quantum dots. A versatile code based on continuum elasticity and 14 band **k·p** theory for zincblende type structures was presented by Marquardt et al. [63] Zhang et al. [54] used a 6×6 **k·p** theory, including piezoelectric and deformation potential effects, to describe, in agreement with experiments, strain-dependent luminescence in wurtzite semiconductor quantum well structures.

Perspective

Besides the rapid progress made in piezotronic research of traditional piezoelectric semiconductors, new quantum materials show good opportunity to obtain ultra-high performance piezotronic and piezo-phototronic devices. Piezoelectric field in two-dimensional non-centrosymmetric materials MoS_2 is demonstrated to modulate the valley and spin magnetoelectricity. Strain-manipulated valleytronic devices show promise for magnetization switching and detection application at room temperature [64]. Recently in quantum acoustics,

piezoelectric semiconductor has shown strong correlation to superconducting qubit due to the large coupling strength of mechanical stimuli and electrical excitations [65]. Piezoelectric field can also be used to manipulate the quantum states of the confined electrons of a gate-controlled quantum dot in GaAs/AlGaAs quantum well, which leads to a high coefficient of electron-to-mechanics coupling [66].

Topological insulators in HgTe/CdTe quantum well structure have been proposed theoretically and verified experimentally [67-69], which holds promise enabling quantum computer with low energy consumption. Recent theoretical results have suggested that the strong piezoelectric field coupling to strain can induce topological insulator states in GaN/InN/GaN quantum well [70]. Strain-induced piezoelectric field can modulate the quantum point contact in HgTe/CdTe and GaN/InN/GaN quantum wells [71, 72]. Based on these understandings, a piezotronic transistor based on topological insulator has been proposed, as shown in figure 4. The ON/OFF conductance ratio is over 10^{10}, offering an excellent switching behaviors [71]. In addition, piezoelectric potential in ZnO/P3HT nanowire array structure can enhance the Rashba spin-orbit interaction at room temperature [73]. The modulation of spin transport offers strain-gated high performance spin devices with low energy consumption, and providing a platform for discovering new physics.

Reference

[1] W. Wu, Z.L. Wang, Piezotronics and piezo-phototronics for adaptive electronics and optoelectronics, Nature Reviews Materials, 1 (2016).
[2] Z.L. Wang, Piezopotential gated nanowire devices: Piezotronics and piezo-phototronics, Nano Today, 5 (2010) 540-552.
[3] Z.L. Wang, Piezotronics and Piezo-Phototronics, Springer: Berlin, 2013.
[4] Z.L. Wang, J.H. Song, Piezoelectric nanogenerators based on zinc oxide nanowire arrays, Science, 312 (2006) 242-246.
[5] Z.L. Wang, Nanogenerators and nanopiezotronics, Int El Devices Meet, (2007) 371-374.
[6] Y. Qin, X. Wang, Z.L. Wang, Microfibre-nanowire hybrid structure for energy scavenging, Nature, 451 (2008) 809-813.
[7] X. Wang, J. Zhou, J. Song, J. Liu, N. Xu, Z.L. Wang, Piezoelectric field effect transistor and nanoforce sensor based on a single ZnO nanowire, Nano Lett, 6 (2006) 2768-2772.
[8] J. Zhou, Y. Gu, P. Fei, W. Mai, Y. Gao, R. Yang, G. Bao, Z.L. Wang, Flexible piezotronic strain sensor, Nano Lett, 8 (2008) 3035-3040.
[9] Q. Yang, W. Wang, S. Xu, Z.L. Wang, Enhancing light emission of ZnO microwire-based diodes by piezo-phototronic effect, Nano letters, 11 (2011) 4012-4017.
[10] D.Q. Zheng, Z.M. Zhao, R. Huang, J.H. Nie, L.J. Li, Y. Zhang, High-performance piezo-phototronic solar cell based on two-dimensional materials, Nano Energy, 32 (2017) 448-453.
[11] W. Wu, X. Wen, Z.L. Wang, Taxel-addressable matrix of vertical-nanowire piezotronic transistors for active and adaptive tactile imaging, Science, 340 (2013) 952-957.
[12] C. Pan, L. Dong, G. Zhu, S. Niu, R. Yu, Q. Yang, Y. Liu, Z.L. Wang, High-resolution electroluminescent imaging of pressure distribution using a piezoelectric nanowire LED array, Nature Photonics, 7 (2013) 752-758.
[13] W. Wu, L. Wang, Y. Li, F. Zhang, L. Lin, S. Niu, D. Chenet, X. Zhang, Y. Hao, T.F. Heinz, J. Hone, Z.L. Wang, Piezoelectricity of single-atomic-layer MoS2 for energy conversion and piezotronics, Nature, 514 (2014) 470-474.
[14] W. Wu, Y. Wei, Z.L. Wang, Strain-gated piezotronic logic nanodevices, Adv Mater, 22 (2010) 4711-4715.
[15] Y. Zhang, Y. Liu, Z.L. Wang, Fundamental theory of piezotronics, Adv Mater, 23 (2011) 3004-3013.
[16] Y. Zhang, Z.L. Wang, Theory of piezo-phototronics for light-emitting diodes, Adv Mater, 24 (2012) 4712-4718.
[17] Y. Zhang, Y. Yang, Z.L. Wang, Piezo-phototronics effect on nano/microwire solar cells, Energ Environ Sci, 5 (2012) 6850-6856.
[18] Y. Liu, Y. Zhang, Q. Yang, S. Niu, Z.L. Wang, Fundamental theories of piezotronics and piezo-phototronics, Nano Energy, 14 (2015) 257-275.
[19] P. Zhu, Z. Zhao, J. Nie, G. Hu, L. Li, Y. Zhang, Ultra-high sensitivity strain sensor based on piezotronic bipolar transistor, Nano Energy, 50 (2018) 744-749.
[20] K. Gu, D.Q. Zheng, L.J. Li, Y. Zhang, High-efficiency and stable piezo-phototronic organic perovskite solar cell, Rsc Adv, 8 (2018) 8694-8698.
[21] K.W. Chung, Z. Wang, J.C. Costa, F. Williamson, P.P. Ruden, M.I. Nathan, Barrier Height Change in Gaas Schottky Diodes Induced by Piezoelectric Effect, Appl Phys Lett, 59 (1991) 1191-1193.
[22] M. Mitra, J. Drayton, M.L.C. Cooray, V.G. Karpov, D. Shvydka, Piezo-photovoltaic coupling in CdS-based thin-film photovoltaics, J Appl Phys, 102 (2007).
[23] F. Boxberg, N. Sondergaard, H.Q. Xu, Photovoltaics with piezoelectric core-shell nanowires, Nano Lett, 10 (2010) 1108-1112.
[24] J.H. Nie, G.W. Hu, L.J. Li, Y. Zhang, Piezotronic analog-to-digital converters based on strain-gated transistors, Nano Energy, 46 (2018) 423-427.
[25] Y. Hu, Y. Zhang, Y. Chang, R.L. Snyder, Z.L. Wang, Optimizing the power output of a ZnO photocell by piezopotential, ACS Nano, 4 (2010) 4220-4224.
[26] S.M. Sze, Physics of semiconductor devices, Wiley: New York, 1981.
[27] T. Ikeda, Fundamentals of Piezoelectricity, Oxford University Press, Oxford UK, 1996.

[28] G.A. Maugin, Continuum Mechanics of Electromagnetic Solids, North-Holland, Amsterdam, 1988.
[29] R.W. Soutas-Little, Elasticity, XVI, 431, Dover Publications, Mineola, NY, 1999.
[30] L. Luo, Y. Zhang, L.J. Li, Piezotronic PIN diode for microwave and piezophototronic devices, Semicond Sci Tech, 32 (2017).
[31] L.S. Jin, X.H. Yan, X.F. Wang, W.J. Hu, Y. Zhang, L.J. Li, Dynamic model for piezotronic and piezo-phototronic devices under low and high frequency external compressive stresses, J Appl Phys, 123 (2018).
[32] K. Natori, Ballistic metal‐oxide‐semiconductor field effect transistor, Journal of Applied Physics, 76 (1994) 4879-4890.
[33] Y. Zhang, L.J. Li, Piezophototronic effect enhanced luminescence of zinc oxide nanowires, Nano Energy, 22 (2016) 533-538.
[34] L.J. Li, Y. Zhang, Simulation of wavelength selection using ZnO nanowires array, J Appl Phys, 121 (2017).
[35] L.J. Li, Y. Zhang, Controlling the luminescence of monolayer MoS2 based on the piezoelectric effect, Nano Res, 10 (2017) 2527-2534.
[36] X. Huang, C. Jiang, C. Du, L. Jing, M. Liu, W. Hu, Z.L. Wang, Enhanced Luminescence Performance of Quantum Wells by Coupling Piezo-Phototronic with Plasmonic Effects, ACS nano, 10 (2016) 11420-11427.
[37] C. Jiang, L. Jing, X. Huang, M. Liu, C. Du, T. Liu, X. Pu, W. Hu, Z.L. Wang, Enhanced Solar Cell Conversion Efficiency of InGaN/GaN Multiple Quantum Wells by Piezo-Phototronic Effect, ACS nano, 11 (2017) 9405-9412.
[38] R. Baraki, N. Novak, T. Fromling, T. Granzow, J. Rodel, Bulk ZnO as piezotronic pressure sensor, Appl Phys Lett, 105 (2014).
[39] H.D. Espinosa, R.A. Bernal, M. Minary-Jolandan, A review of mechanical and electromechanical properties of piezoelectric nanowires, Adv Mater, 24 (2012) 4656-4675.
[40] Y.J. Lei, Y.S. Leng, Molecular Simulation of Metal-ZnO Contact in ZnO Piezoelectric Nanogenerator, Int Conf Manip Manu, (2013) 291-294.
[41] D. Tan, Y. Xiang, Y. Leng, Molecular Simulation Study of Piezoelectric Potential Distribution in a ZnO Nanowire under Mechanical Bending, MRS Advances, 2 (2017) 3433-3439.
[42] D. Tan, Y. Xiang, Y. Leng, Y. Leng, On the metal/ZnO contacts in a sliding-bending piezoelectric nanogenerator, Nano Energy, 50 (2018) 291-297.
[43] E.J. Reed, M.R. Armstrong, K.Y. Kim, J.H. Glownia, Atomic-scale time and space resolution of terahertz frequency acoustic waves, Physical review letters, 101 (2008) 014302.
[44] S. Dai, M.L. Dunn, H.S. Park, Piezoelectric constants for ZnO calculated using classical polarizable core-shell potentials, Nanotechnology, 21 (2010) 445707.
[45] J. Zhang, J. Zhou, Humidity-dependent piezopotential properties of zinc oxide nanowires: Insights from atomic-scale modelling, Nano Energy, 50 (2018) 298-307.
[46] Z. Zhou, D. Qian, M. Minary-Jolandan, Molecular Mechanism of Polarization and Piezoelectric Effect in Super-Twisted Collagen, Acs Biomater Sci Eng, 2 (2016) 929-936.
[47] B. Huang, Native Point Defects in CaS: Focus on Intrinsic Defects and Rare Earth Ion Dopant Levels for Up-converted Persistent Luminescence, Inorganic chemistry, 54 (2015) 11423-11440.
[48] B.L. Huang, M.Z. Sun, D.F. Peng, Intrinsic energy conversions for photon-generation in piezo-phototronic materials: A case study on alkaline niobates, Nano Energy, 47 (2018) 150-171.
[49] B. Huang, Doping of RE ions in the 2D ZnO layered system to achieve low-dimensional upconverted persistent luminescence based on asymmetric doping in ZnO systems, Physical chemistry chemical physics : PCCP, 19 (2017) 12683-12711.
[50] H. Momida, T. Oguchi, Effects of lattice parameters on piezoelectric constants in wurtzite materials: A theoretical study using first-principles and statistical-learning methods, Appl Phys Express, 11 (2018).
[51] W. Liu, A.H. Zhang, Y. Zhang, Z.L. Wang, First principle simulations of piezotronic transistors, Nano Energy, 14 (2015) 355-363.
[52] W. Liu, A. Zhang, Y. Zhang, Z.L. Wang, Density functional studies on wurtzite piezotronic transistors: influence of different semiconductors and metals on piezoelectric charge distribution and Schottky barrier, Nanotechnology, 27 (2016) 205204.
[53] R. Hinchet, U. Khan, C. Falconi, S.-W. Kim, Piezoelectric properties in two-dimensional materials: Simulations and experiments, Materials Today, (2018).

[54] A.H. Zhang, M.Z. Peng, M. Willatzen, J.Y. Zhai, Z.L. Wang, Piezoelectric and deformation potential effects of strain-dependent luminescence in semiconductor quantum well structures, Nano Res, 10 (2017) 134-144.
[55] H.Y. Zhu, Y. Wang, J. Xiao, M. Liu, S.M. Xiong, Z.J. Wong, Z.L. Ye, Y. Ye, X.B. Yin, X. Zhang, Observation of piezoelectricity in free-standing monolayer MoS2, Nature nanotechnology, 10 (2015) 151-155.
[56] R.X. Fei, W.B. Li, J. Li, L. Yang, Giant piezoelectricity of monolayer group IV monochalcogenides: SnSe, SnS, GeSe, and GeS, Appl Phys Lett, 107 (2015).
[57] Y. Yan, J.E. Zhou, D. Maurya, Y.U. Wang, S. Priya, Giant piezoelectric voltage coefficient in grain-oriented modified PbTiO3 material, Nature communications, 7 (2016) 13089.
[58] L.C.L.Y. Voon, M. Willatzen, Electromechanical phenomena in semiconductor nanostructures, J Appl Phys, 109 (2011).
[59] D. Barettin, S. Madsen, B. Lassen, M. Willatzen, Computational Methods for Electromechanical Fields in Self-Assembled Quantum Dots, Commun Comput Phys, 11 (2012) 797-830.
[60] M. Grundmann, O. Stier, D. Bimberg, InAs/GaAs pyramidal quantum dots: Strain distribution, optical phonons, and electronic structure, Physical review. B, Condensed matter, 52 (1995) 11969-11981.
[61] A.D. Andreev, E.P. O'Reilly, Theory of the electronic structure of GaN/AlN hexagonal quantum dots, Phys Rev B, 62 (2000) 15851-15870.
[62] V.A. Fonoberov, A.A. Balandin, Excitonic properties of strained wurtzite and zinc-blende GaN/AlxGa1-xN quantum dots, J Appl Phys, 94 (2003) 7178-7186.
[63] O. Marquardt, S. Boeck, C. Freysoldt, T. Hickel, S. Schulz, J. Neugebauer, E.P. O'Reilly, A generalized plane-wave formulation of k p formalism and continuum-elasticity approach to elastic and electronic properties of semiconductor nanostructures, Computational Materials Science, 95 (2014) 280-287.
[64] J. Lee, Z. Wang, H. Xie, K.F. Mak, J. Shan, Valley magnetoelectricity in single-layer MoS2, Nat Mater, 16 (2017) 887-891.
[65] Y. Chu, P. Kharel, W.H. Renninger, L.D. Burkhart, L. Frunzio, P.T. Rakich, R.J. Schoelkopf, Quantum acoustics with superconducting qubits, Science, 358 (2017) 199-202.
[66] Y. Okazaki, I. Mahboob, K. Onomitsu, S. Sasaki, H. Yamaguchi, Gate-controlled electromechanical backaction induced by a quantum dot, Nature communications, 7 (2016) 11132.
[67] B.A. Bernevig, T.L. Hughes, S.C. Zhang, Quantum spin Hall effect and topological phase transition in HgTe quantum wells, Science, 314 (2006) 1757-1761.
[68] M. Konig, S. Wiedmann, C. Brune, A. Roth, H. Buhmann, L.W. Molenkamp, X.L. Qi, S.C. Zhang, Quantum spin hall insulator state in HgTe quantum wells, Science, 318 (2007) 766-770.
[69] C.Z. Chang, J. Zhang, X. Feng, J. Shen, Z. Zhang, M. Guo, K. Li, Y. Ou, P. Wei, L.L. Wang, Z.Q. Ji, Y. Feng, S. Ji, X. Chen, J. Jia, X. Dai, Z. Fang, S.C. Zhang, K. He, Y. Wang, L. Lu, X.C. Ma, Q.K. Xue, Experimental observation of the quantum anomalous Hall effect in a magnetic topological insulator, Science, 340 (2013) 167-170.
[70] M.S. Miao, Q. Yan, C.G. Van de Walle, W.K. Lou, L.L. Li, K. Chang, Polarization-driven topological insulator transition in a GaN/InN/GaN quantum well, Physical review letters, 109 (2012) 186803.
[71] G. Hu, Y. Zhang, L. Li, Z.L. Wang, Piezotronic Transistor Based on Topological Insulators, ACS Nano, 12 (2018) 779-785.
[72] M. Dan, G. Hu, L. Li, Y. Zhang, High performance piezotronic logic nanodevices based on GaN/InN/GaN topological insulator, Nano Energy, 50 (2018) 544-551.
[73] L. Zhu, Y. Zhang, P. Lin, Y. Wang, L. Yang, L. Chen, L. Wang, B. Chen, Z.L. Wang, Piezotronic Effect on Rashba Spin-Orbit Coupling in a ZnO/P3HT Nanowire Array Structure, ACS Nano, 12 (2018) 1811-1820.

Figure captions:

Figure 1. (a) Schematic of metal-semiconductor contact based piezotronic transistor. (b) The current-voltage characteristics of the ideal metal-semiconductor contact under different applied strain. (c) Gauge factor as a function of strain for high-sensitivity piezotronic bipolar transistor. (d) The capacitance and frequency response versus the strain in piezotronic PIN diode for microwave applications.

Figure 2. Material properties calculations and device simulations of piezotronics and piezo-phototronics. Elastic and piezoelectric properties including crystal structure, dopant type and grown direction is inputted to atomistic simulation based on mechanical and electronmechanical modeling. Molecular dynamics and density functional theory, as two basic simulation tools are used to calculate the changes induced by the piezoelectric effect and further determine material properties.

Figure 3. (a) Schematic of the piezoelectric effect on ZnO nanowire based on molecular dynamic simulation. (b) The smith-charts are shown by a range of 15 lanthanide dopant ions in ZnO for modulating the output emission luminescence properties. (c) First-principle simulation modeling Ag-ZnO-Ag piezotronic transistor to calculate piezoelectric potential, piezoelectric charges distribution and Schottky barrier heights.

Figure 4. (a) Schematic of piezotronic effect on HgTe/CdTe/HgTe topological insulator and corresponding band structures. (b) Piezotronic effect on transport property of topological insulator based on different piezoelectric materials. Left plane: transport conductance plateaus varying with shear strain. Right plane: electronic density distribution in OFF and ON states is plotted for narrow and wide QPC width, respectively.

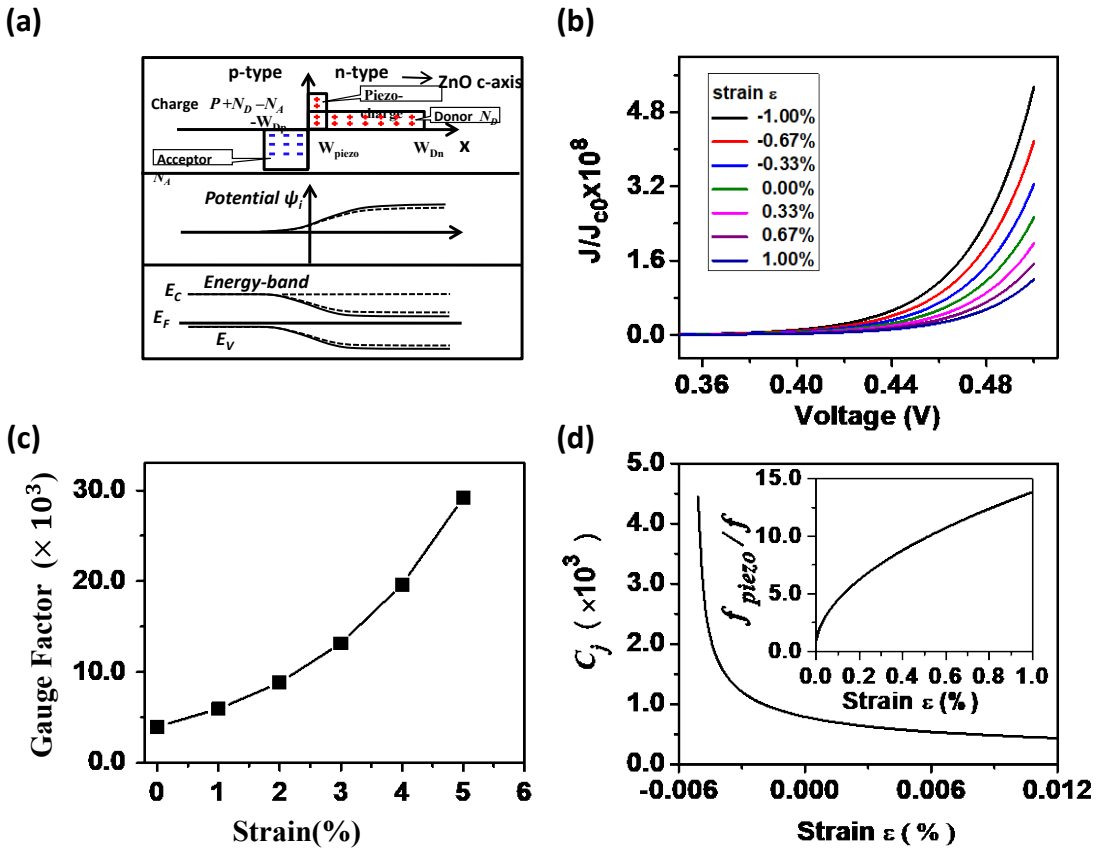
(a)
p-type
n-type
ZnO c-axis
Charge
Piezo-charge
Donor N_D
Acceptor
N_A
W_{Dp}
W_{piezo}
W_{Dn}
x
Potential ψ_i
Energy-band
E_C
E_F
E_V
(b)
strain ε
-1.00%
-0.67%
-0.33%
0.00%
0.33%
0.67%
1.00%
$J/J_{c0}x10^8$
Voltage (V)
(c)
Gauge Factor ($\times 10^3$)
Strain(%)
(d)
C_j ($\times 10^3$)
f_{piezo}/f
Strain ε (%)
Strain ε (%)

Figure 1

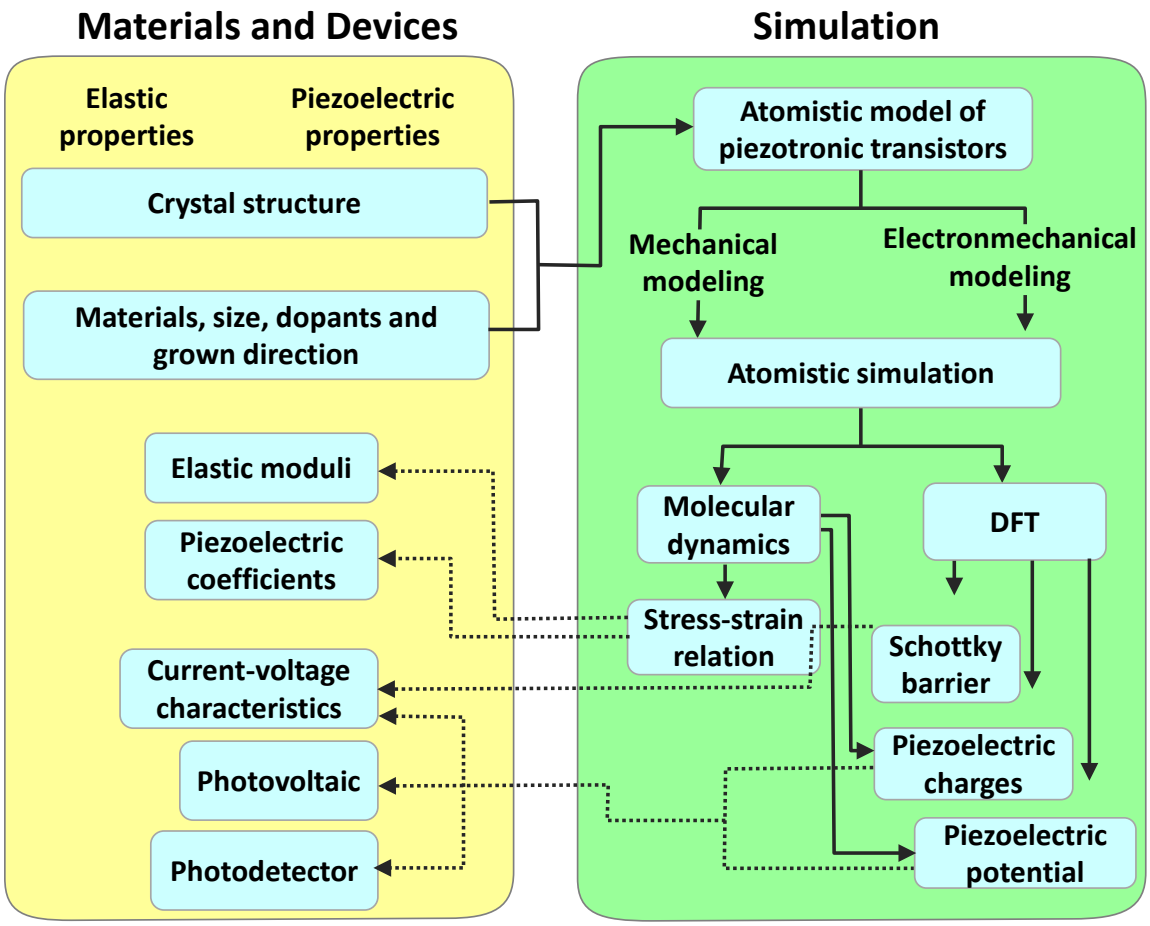
Materials and Devices
Simulation
Elastic properties
Piezoelectric properties
Crystal structure
Materials, size, dopants and grown direction
Elastic moduli
Piezoelectric coefficients
Current-voltage characteristics
Photovoltaic
Photodetector
Atomistic model of piezotronic transistors
Mechanical modeling
Electronmechanical modeling
Atomistic simulation
Molecular dynamics
DFT
Stress-strain relation
Schottky barrier
Piezoelectric charges
Piezoelectric potential

Figure 2

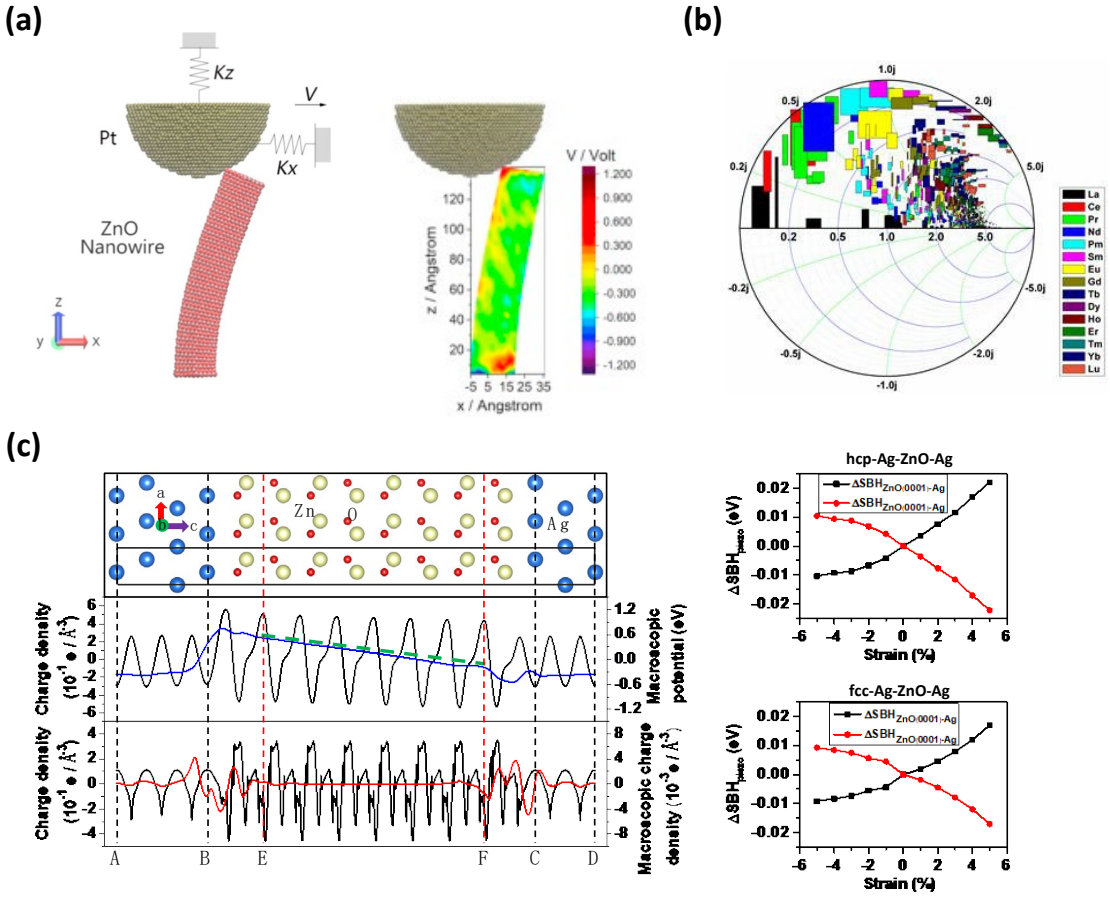
(a)
Kz
V
Pt
Kx
ZnO
Nanowire
z
y
x
V / Volt
1.200
0.900
0.600
0.300
0.000
-0.300
-0.600
-0.900
-1.200
z / Angstrom
x / Angstrom
(b)
La
Ce
Pr
Nd
Pm
Sm
Eu
Gd
Tb
Dy
Ho
Er
Tm
Yb
Lu
(c)
a
c
Zn
O
Ag
Charge density
Macroscopic potential (eV)
Macroscopic charge density
A
B
E
F
C
D
hcp-Ag-ZnO-Ag
fcc-Ag-ZnO-Ag
Strain (%)

Figure 3

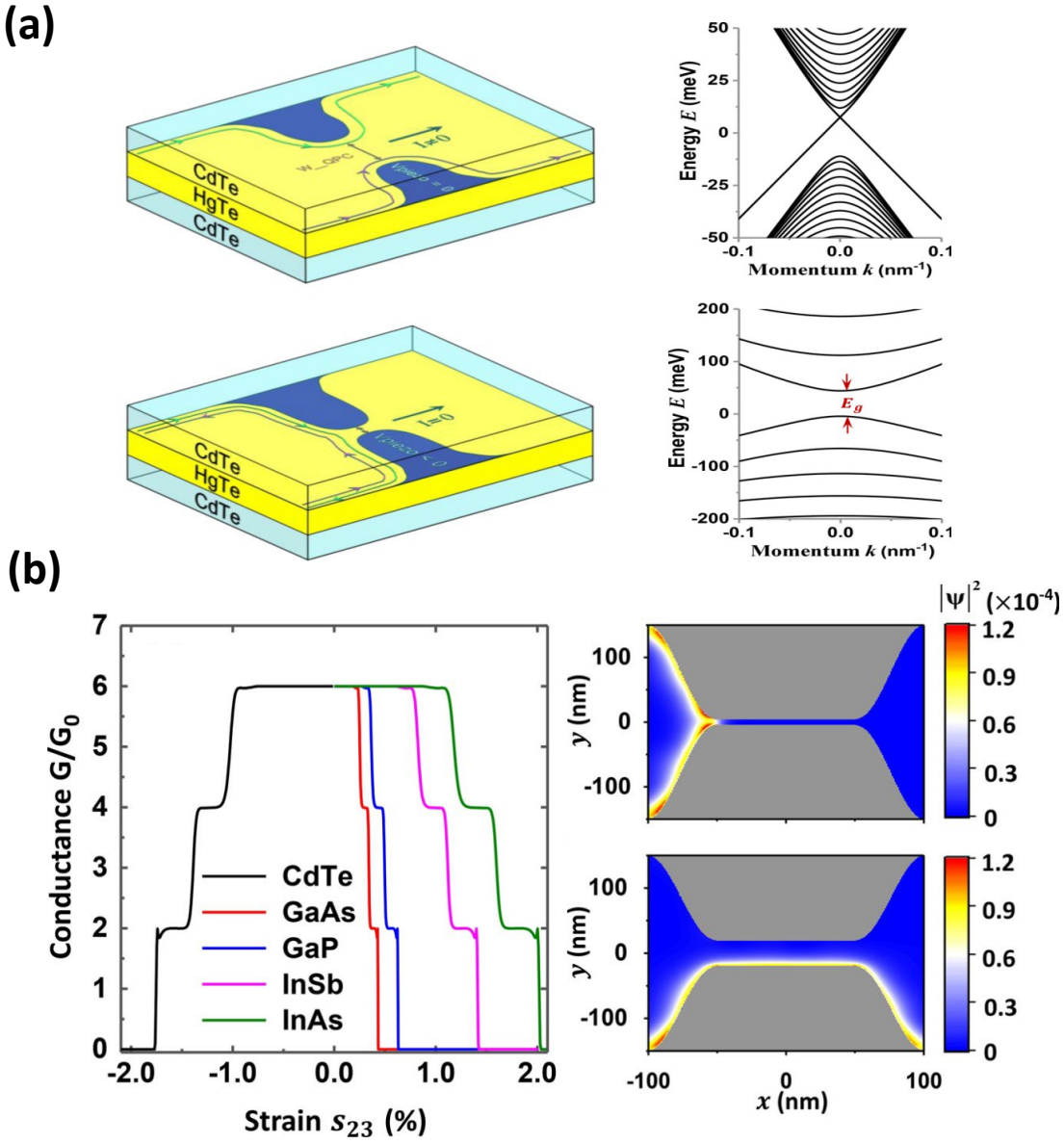
(a)
CdTe
HgTe
CdTe
Energy E (meV)
Momentum k (nm⁻¹)
E_g
(b)
Conductance G/G0
Strain s23 (%)
CdTe
GaAs
GaP
InSb
InAs
|Ψ|² (×10⁻⁴)
y (nm)
x (nm)

Figure 4